## Identification of skeleton-innervating peripheral sensory neurons and their role in fracture repair

Mingxin Xu<sup>1</sup>, Neelima Thottappillil<sup>1</sup>, Masnsen Cherief <sup>1</sup>, Zhao Li<sup>1</sup>, Manyu Zhu<sup>1</sup>, Xin Xing<sup>1</sup>, Mario Gomez-Salazar<sup>1</sup>, Robert Tower<sup>2</sup>, Ziyi Wang<sup>1</sup>, Qizhi Qin<sup>1</sup>, Ray Cheng<sup>3</sup>, Patrick Cahan<sup>3</sup>, Thomas L. Clemens<sup>4</sup>, Aaron W. James<sup>1</sup>

Department of Pathology, Johns Hopkins University, Baltimore, MD, 21205, USA.

<sup>2</sup>Center for Organogenesis and Trauma, Department of Surgery, University of Texas Southwestern, Dallas, TX, USA.

<sup>3</sup>Department of Biomedical Engineering; Institute for Cell Engineering, Johns Hopkins University, Baltimore, MD 21205, USA.

<sup>4</sup>Department of Orthopaedics, University of Maryland School of Medicine, Baltimore, MD 21201.

Presenter Email: mxxu95@gmail.com

**Disclosures:** AWJ is a consultant for Novadip Biosciences and Lifesprout LLC.

INTRODUCTION: Bone is highly innervated by sensory nerves, predominantly on the periosteum. Prior work from our group has shown that proper fracture healing requires intact tropomyosin receptor kinase A (TrkA) signaling, which is mainly expressed on sensory nerves<sup>1</sup>. The specific neuroregulatory molecules important in nerve-bone crosstalk are poorly understood, which is hampered by our lack of understanding of skeletal-innervating neurons, their identity and transcriptional heterogeneity. Here, we utilize a combination of peripheral nerve retrograde tracing and single cell RNA sequencing (scRNA-Seq) to better define the identity of skeletal-innervating neurons as well as their response to bone fracture.

METHODS: To identify skeleton-innervating neurons, an engineered virus with enhanced tropism for peripheral neurons was injected into the midshaft of the ulnar periosteum of 14-week-old mice (3.5µl AAV-PHP.S-tdTomato). 4 weeks after injection, retrograde labeling of dorsal root ganglion (DRG) neurons with AAV-PHP.S-tdTomato was evaluated using whole-mount immunohistochemistry, scRNA-Seq and RNAscope (DRGs at C7, C8, T1 levels were used corresponding to the innervation pattern of the forelimb). To characterize temporal transcriptomic responses to ulnar stress fracture<sup>1</sup>, retrogradely labeled whole DRGs were harvested and dissociated at 1-, 14- and 56- days post-stress fracture and subjected to scRNA-Seq (**Fig1.A**). To uncover ulna callus resident cells that may interact with ulna-innervating sensory neurons, scRNA-Seq of the fracture callus was generated 14 days post-injury. Interaction modalities were performed to reveal potential skeleton-innervating neuron-derived ligands that are involved in fracture repair. All animals were housed and procedures were performed with the approval of the IACUC of Johns Hopkins University.

RESULTS SECTION: Whole mount imaging showed successful retrograde labeling of AAV.PHP.S-tdTomato of DRG (**Fig1.B**). scRNA-Seq profiling of DRGs recovered 6,648 neurons from all time points, consisting of 14 neuronal cell types (**Fig.1C**). Of which, 5.8% were labeled by AAV-PHP.S-tdTomato(tdT<sup>pos</sup>). tdT<sup>pos</sup> neurons were mostly enriched in CGRP-expressing subclusters and low-threshold mechanosensory (LTMR) neurons, with the top 5 clusters being CGRP-Gamma/Beta (17.2%), CGRP-Eta (17.1%), CGRP-Zeta (14.2%), Proprioceptors (10.9%) and Aβ Field-LTMRs (9.2%) (**Fig.1D**), validated by RNAscope (**Fig1.E**). GO enrichment analysis showed tdT<sup>pos</sup> neurons were involved in endochondral ossification, bone mineralization and angiogenesis when compared to tdT<sup>neg</sup> neurons (**Fig.1F-G**). We also compared transcriptomic changes over time to reveal temporal neuronal responses to fracture injury. GO enrichment showed that DRG neurons were mostly involved in sensory perception of pain, signal transduction and immune responses at d1, and skeletal development, cell proliferation and angiogenesis at d14 (**Fig1.H**). Of note, tdT<sup>pos</sup> neurons responded more drastically than tdT<sup>neg</sup> neurons, with 2% of genes significantly dysregulated among labeled neurons, whereas <0.1% of genes changed among non-labeled neurons. To understand if DRG neurons responded differently to peripheral axon injury and bone injury, we compared our data with an available dataset that investigated transcriptomic changes in DRG neurons after nerve injury (SNI)<sup>2</sup>. Differential expressed genes (DEGs) showed little overlap between SNI and fracture injury (**Fig.11**). Classic neuronal injury markers like Atf3, Sox1 and Jun were significantly increased after SNI, however, remained the same after fracture (**Fig.1J**), suggesting a distinct response of sensory neurons to these two types of injury. Interactome modalities were performed to discern potential signaling pathways that may be involved in fracture repair. Several candidates were predicted, for example, FGF and HH

DISCUSSION: By integrating retrograde labeling and dorsal root ganglia scRNA-seq, we mapped peripheral sensory neurons that innervate long bones. Skeleton-innervating neurons were mostly CGRP subclusters and LTMR neurons, corresponding to their function of sensory perception of pain and mechanical force. Also, they were markedly molecularly distinct from non-skeleton-innervating neurons. Dynamic temporal transcriptomic changes were observed in sensory neurons during the fracture repair process, with gene ontology suggesting pain sensation and immune responses during acute phase and functions such as regulation of cell proliferation, ossification and angiogenesis during later phases. Interactome analysis between DRG neurons and callus resident cells suggested that skeleton-innervating neurons may be involved in fracture repair by secreting specific neuroregulatory ligands.

 $SIGNIFICANCE/CLINICAL\ RELEVANCE:\ This\ study\ identified\ skeleton-innervating\ neurons\ and\ characterized\ how\ they\ responded\ to\ bone\ fracture\ injury.$ 

REFERENCES: 1. Zhu, L., et al. (2019). J Clin Invest 129(12):5137-5150. 2. Wang, K., et al. (2021). Cell Res 31(8): 904-918.

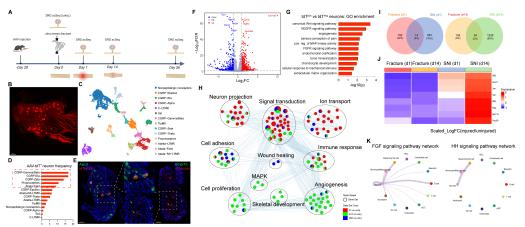


Figure 1: (A) Schematic diagram of the experiment. **(B)** Whole mount staining of C7 DRG at 4 weeks after ulna periosteum injection of AAV.PHP.S. (C) UMAP of DRG neurons, colored by cell types. (D) Percentage of tdT<sup>pos</sup> neurons in each cell type. Dash box shows top 5 clusters. (E) RNA scope validation of colocalization of tdTomato and CGRP-Eta, CGRP-Zeta markers. (F) Volcano plot of comparison between tdT<sup>pos</sup> vs tdT<sup>neg</sup> neurons at baseline. (G) GO enrichment in tdT<sup>pos</sup> neurons. (H) Enrichment map displays the significantly enriched gene-sets in neurons post injury vs. uninjured condition. Nodes represent gene-sets and edges represent GO defined relations. Clusters are annotated according to the corresponding function. (I) Venn diagram of DEGs numbers and percentages between fracture and SNI injury. (J) Heatmap of common injury marker genes expression in DRG neurons after fracture and SNI injury at d1 and d14. (K) FGF and HH signaling pathway network between DRG neurons and callus resident cells.